

# A Study on the Measurement Method of Spatial Position Compensation for Virtual Reality and Real Space Synchronization

Kee-Jin Park<sup>\*,\*\*\*\*</sup>, Byoung-Hwak Lee<sup>\*\*</sup>, Nam-Hyuk Kim<sup>\*\*\*</sup>, Sung-Ho Yoon<sup>\*\*\*\*,#</sup>

<sup>\*</sup>Daegu Mechatronics & Materials Institute,

<sup>\*\*</sup>Department of Physics & Chemistry, Korea Military Academy, <sup>\*\*\*</sup>Optimus System LTD,

<sup>\*\*\*\*</sup>Department of Mechanical Engineering, Kumoh national Institute of Technology.

## 가상현실과 실공간 동기화를 위한 공간 위치보정 측정 방법론에 대한 연구

박기진<sup>\*,\*\*\*\*</sup>, 이병학<sup>\*\*</sup>, 김남혁<sup>\*\*\*</sup>, 윤성호<sup>\*\*\*\*,#</sup>

<sup>\*</sup>대구기계부품연구원, <sup>\*\*</sup>육군사관학교, <sup>\*\*\*</sup>옵티머스시스템(주), <sup>\*\*\*\*</sup>금오공과대학교 기계공학과

(Received 31 October 2018; received in revised form 13 November 2018; accepted 19 November 2018)

### ABSTRACT

Recently, with the rapid development of virtual reality technology, there have been more and more applications of virtual reality technology in various fields. In order to realize a virtual reality, a method of implementing a visualization environment through an HMD (Head Mounted Display) is widely used. However, in the current visualization environment through the HMD, the user feels dizziness when worn, It has the disadvantage of imposing restrictions on. In this study, it is aimed to realize virtual reality visualization environment through multi-screen environment which improves the experience effect of virtual environment by using existing screen instead of visualization through HMD, and compensates for shortcomings of HMD method. In order to realize a multi-screen environment as a highly visualized environment, a technique for matching the spatial position of the multi-screen with the spatial position of the virtual environment is required. To do this, we need an efficient method to precisely measure the position of the space, and we propose a spatial position compensation methodology that can efficiently and precisely measure the position of the real space and reflect it in the virtual environment.

**Key Words** : Space Synchronization(공간동기화) Motion Tracking(모션트래킹), Virtual Environment(가상환경), Simulator(시뮬레이터), Structural Analysis(구조해석)

### 1. Introduction

With the rapid development in virtual reality

(VR) technology in recent years, VR has been increasingly applied in a wide variety of areas. To implement VR, a method to realize visualization environments through head-mounted displays (HMDs) has been widely used. However, the

# Corresponding Author : shyoon@kumoh.ac.kr

Tel: +82-54-478-7041, Fax: +82-54-478-7064

visualization environment implemented through HMDs has drawbacks in that it may cause dizziness in users or limits users' behavior as the HMD blocks their eyes<sup>[1-2]</sup>. This study aims to implement VR visualization environments through a multi-surface and multi-screen environment that can overcome the drawbacks of the HMD method and increase the realistic effect of virtual environment using existing screens. To implement the multi-screen method as a realistic visualization environment, a technique is needed to match the spatial location in the multi-screen with that in the virtual environment. To do this, an efficient method that can measure the spatial location precisely is needed, and a methodology for spatial location correction that reflects the measurement of real space location efficiently and precisely to the virtual environment is presented in this study.

## 2. Concept of synchronization of virtual and real spaces

Fig. 1 shows the theoretical conceptual diagram of synchronization between virtual and real spaces. Fig. 2 shows the definition of the synchronization method between virtual and real spaces, which measures the spatial reference location and the multi-screen's location in the multi-screen environment of real space precisely and matches them with the reference location in the virtual environment.

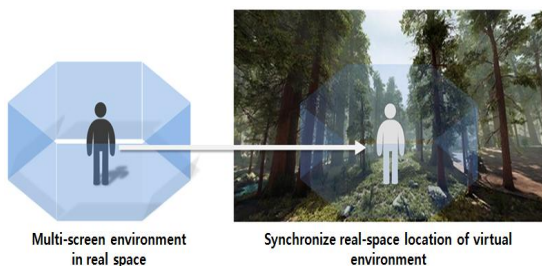


Fig. 1 Concept of space synchronization

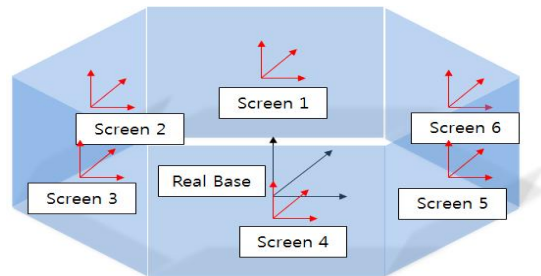


Fig. 2 Defining the coordinate system of a multi-screen

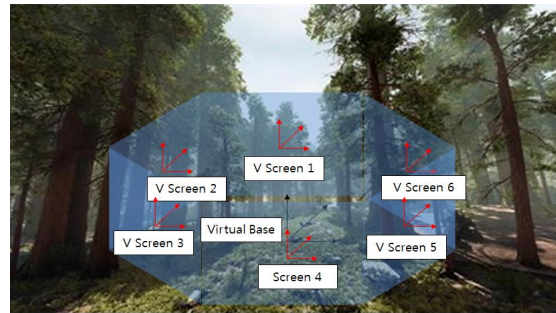


Fig. 3 Defining the coordinate system of a virtual space

As shown in Fig. 3, the user's location in the virtual space can be synchronized by reflecting the multi-screen's location to the virtual environment. The real and virtual spaces can be precisely synchronized by efficiently configuring the multi-screen environment, which is a real space, and reflecting the screen location and direction accurately to the virtual environment. To implement this, a stable multi-screen structure is required, as well as a measurement method to reflect the screen location accurately.

## 3. Design of the simulator main frame structure

### 3.1 Finite element modeling and analysis conditions

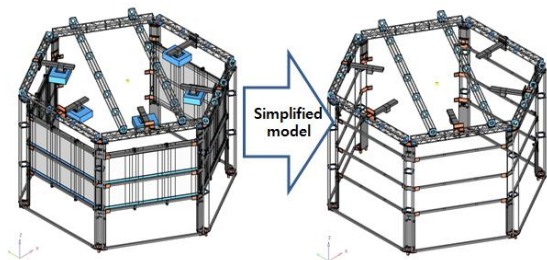


Fig. 4 Simplified analysis model for main frame

Table 1 Material of properties for analysis model

Material	Modulus of elasticity (MPa)	Poisson's ratio	Density (g/cm <sup>3</sup> )	Yield strength (MPa)
Aluminium	69,000	0.33	2.70	55
Steel	210,000	0.30	7.87	230

The deformation due to self-weight of the simulator main frame of a VR technology-applied multi-screen structure should be minimized for accurate mapping of real and virtual spaces. Fig. 4 shows a simplified model for static stiffness analysis and three-dimensional (3D) design shape of the main frame. Here, small parts were omitted and small grooves and edge parts that did not significantly affect the analysis were simplified, considering that a frame is assembled using bolts and nuts by part<sup>[3-5]</sup>. To create the finite element model, the connection and support portions of each structure were divided into tetra elements, which became solid elements using HyperMesh, and the profile was divided using the Quad or sheet element. The length of each side of the finite element model was set to 5 mm as the basic length.

Table 1 presents the physical properties of the materials used in the analysis model. Here, the profile part was made from aluminum, and the connecting and supporting portions were made from steel. An integrated shape was assumed considering that the contact surface of each part was assembled by bolts. For the boundary condition for static stiffness

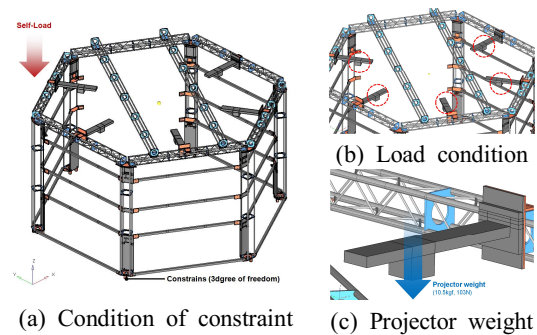


Fig. 5 Stiffness analysis condition for main frame

analysis of the frame, a three-degree freedom constraint was applied to the bottom support surface as shown in Fig. 5(a), and a loading condition of 10.5 kg was applied to each of the five projectors mounted on the upper side of the simulator as shown in Figs. 5(B) and 5(c). The stress and strain distribution due to self-weight were analyzed at the frame's entire assembly condition using Hyperworks Optistruct based on the above analysis conditions.

### 3.2 Results of static stiffness analysis

Fig. 6 shows the results of the static stiffness analysis on the frame's stress distribution according to the self-weight and the projector's load. The maximum stress was 28.2 MPa, indicating that the stress was concentrated on the support frame in the upper projector. However, the stress was below the yield strength of the aluminum (55 MPa), which indicated no problem in static stiffness. In addition, the design safety factor was 1.7 times or higher, which also demonstrated that the structural safety was secured. Fig. 7 shows the results of the static stiffness analysis on the frame's strain distribution according to the self-weight and the projector's load. The maximum strain was 1.17 mm, which occurred at the end of the support portion of the projector. The motion recognition precision for precise mapping of the virtual and real spaces was  $\pm 5$  mm, and the maximum strain of the frame, 1.17 mm, did

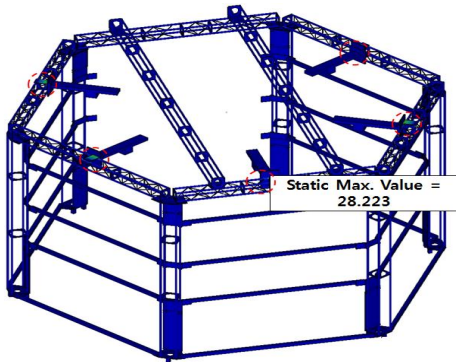


Fig. 6 Stress distribution of stiffness analysis

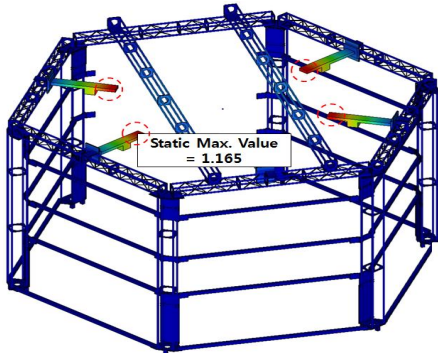


Fig. 7 Displacement distribution of stiffness analysis

not have a significant impact on the location correction of the virtual and real spaces.

#### 4. Measurement method of spatial location of multi-screen

The location of the real space shall be measured precisely and reflected to visualize the virtual environment and synchronize the multi-screen system in real space with that in the virtual space. In particular, 3D precision measurement devices such as laser trackers may be used to measure the multi-screen in real space, but these expensive measurement devices have drawbacks with regard to mobility and inconvenience of use. To overcome

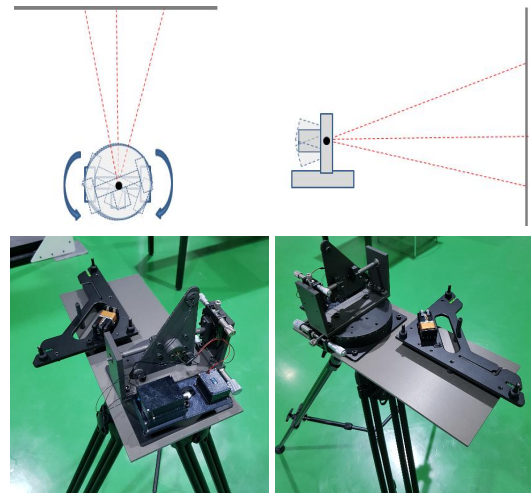


Fig. 8 Degree of freedom for measurement system

these drawbacks, this study developed a measurement device that facilitated easy movements and precision measurements using a sensor applied to the multi-screen, and a measurement algorithm was investigated.

##### 4-1. Development of spatial location measurement device

Fig. 8 shows the schematic design diagram of the two degrees of freedom-based spatial location measurement device, and the actually fabricated device. The location of the multi-screen is measured by projecting a laser beam onto the rotation center of the two degrees of freedom mechanism and placing it in a specific location on the screen surface. In particular, a rotation direction in each rotation axis of the measurement device is read during measurements, and using this rotation value, a relative position and direction between the screen and the measurement device can be obtained.

##### 4-2. Development of spatial location measurement algorithm

Fig. 9 shows the coordinate definition used to measure

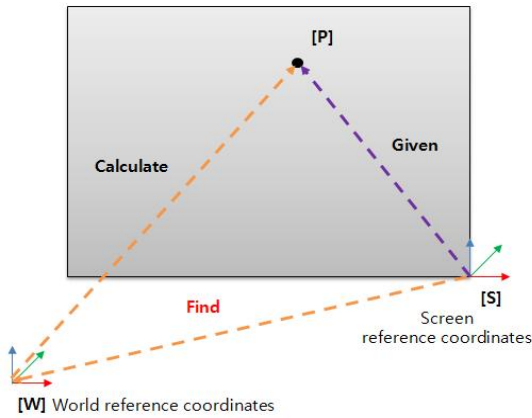


**Fig. 9 Definition of reference coordinate system**

the location and direction of the multi-screen in real space. The value given at the coordinate definition is  ${}_sP_{P_n}$ , which is presented in Eq. (1), and it indicates an arbitrary location value given by the screen reference coordinate.

$${}_sT_W * {}_wP_{P_n} = {}_sP_{P_n} \quad \text{----- (1)}$$

Here,  ${}_sT_W$  refers to the location and direction of the world reference coordinate viewed from the screen reference coordinate,  ${}_wP_{P_n}$  refers to the location of the measurement point above the screen viewed from the world reference coordinate, and  ${}_sP_{P_n}$  refers to the location of the measurement point above the screen viewed from the screen reference coordinate. In addition, the following condition is given for  ${}_sP_{P_n}$ . During measurements, and according to the two measurement conditions, a measurement point is defined according to the method shown in Fig. 10. In particular, each of the points is measured at the fixed location.

condition 1.

During the measurement of  $P_n(P_1, P_2, \dots P_n)$ , three points are measured, and three points should be located in a straight line.

condition 2.

The measurement reference location during the

three-point measurement should be measured by turning the angle only at the fixed state.

condition 3.

$P_1, P_5,$  and  $P_3$  should be located in a straight line.

condition 4.

$P_2, P_5,$  and  $P_4$  should be located in a straight line.

condition 5.

The spatial reference coordinate (W) and measurement reference location (J) are defined identically.

If the triangle made by the measurement reference location J and the measurement point  $P_1$  and  $P_3$  above the screen in Fig. 11 is defined using the location value of each point obtained in the above as shown in Fig. 11, the vectors of  $x_1, x_2,$  and  $x_3$  are first calculated to obtain the rotation angle ( $\theta_1, \theta_2$ ) at the measurement reference location J, thereby calculating the in-between angle using the vector's inner product. Here, the vector values of  $x_1, x_2,$  and  $x_3$  are directional values of the laser pointer that moves from the measurement reference location J plane perpendicularly and employs the three measurement point values ( $P_1, P_5, P_3$ ) at the measurement reference location J. Two vectors over the measurement plane are calculated using the three points. Then, if the outer vector product of these two vectors is calculated, the direction vector of the laser pointer can be calculated. Assuming that the measurement laser pointer's direction at  ${}_wT_1$  and  ${}_wT_5$  is the Z direction, the definitions can be produced as presented in Eqs. (2) to (5)<sup>[6]</sup>.

$$\text{Vector } x_1 = (a_{x1}, a_{y1}, a_{z1}) \quad \text{----- (2)}$$

$$\text{Vector } x_3 = (a_{x5}, a_{y5}, a_{z5}) \quad \text{----- (3)}$$

$$x_1 \cdot x_3 = |x_1| * |x_3| * \cos\theta_1 \quad \text{----- (4)}$$

$$\theta_1 = \text{acos} \left( \frac{(a_{x1} * a_{x5} + a_{y1} * a_{y5} + a_{z1} * a_{z5}) / (\sqrt{a_{x1} * a_{x1} + a_{y1} * a_{y1} + a_{z1} * a_{z1}} * \sqrt{a_{x5} * a_{x5} + a_{y5} * a_{y5} + a_{z5} * a_{z5}})} \right) \quad \text{----- (5)}$$

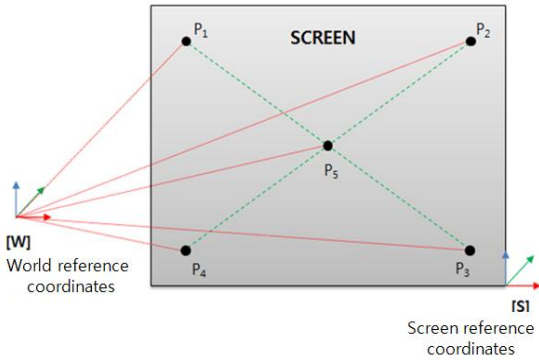


Fig. 10 Definition of measuring position

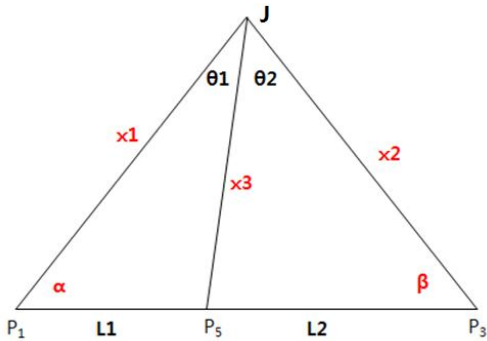


Fig. 11 Relationship between measurement position and vector

$\theta_2$  can also be defined in the same manner, through which  $\theta_1$ ,  $\theta_2$ ,  $L_1$ , and  $L_2$  can be defined. Here,  $x_1$ ,  $x_2$ ,  $x_3$ ,  $\alpha$ , and  $\beta$  can be calculated, and Eqs. (6) to (12) can be defined using the trigonometric function<sup>[7]</sup>.

$$A = (L_1+L_2)/\sin(\theta_1+\theta_2)$$

$$B = L_1/\sin\theta_1$$

$$C = L_2/\sin\theta_2$$

$$x_2 - A * \sin\alpha = 0 \text{ ----- (6)}$$

$$x_1 - A * \sin\beta = 0 \text{ ----- (7)}$$

$$x_3 - B * \sin\alpha = 0 \text{ ----- (8)}$$

$$x_3 - C * \sin\beta = 0 \text{ ----- (9)}$$

$$(x_3)^2 - (x_1)^2 + 2 * L_1 * x_1 * \cos\alpha - (L_1)^2 = 0 \text{ -----(10)}$$

$$(x_3)^2 - (x_2)^2 + 2 * L_2 * x_2 * \cos\beta - (L_2)^2 = 0 \text{ -----(11)}$$

$$(x_1)^2 + (x_2)^2 - 2 * \cos(\theta_1+\theta_2) * x_1 * x_2 - (L_1+L_2)^2 = 0 \text{ -----(12)}$$

Using the above equations, a non-linear equation consisting of five unknown numbers ( $x_1$ ,  $x_2$ ,  $x_3$ ,  $\alpha$ ,  $\beta$ ) and seven equations (Eqs. (6) to (12)) is solved to obtain the distance and angle of each screen. Finally, the reference coordinate location and the direction of the screen viewed from the reference coordinate can be acquired<sup>[8]</sup>.

### 5. Measurement method of spatial location and verification of the device

To verify the reliability of the measurement device and the method developed to measure the spatial location, a testbed was configured utilizing a laser tracker (a 3D precision measurement device) and a screen frame as shown in Fig. 12. Table 2 presents the analysis results after comparing the



Fig. 12 Field measurement experiment

Table 2 Comparison of measurement precision

Type	x	y	z	yaw	pitch	roll
Laser tracker	908.011	11.579	-95.413	0.024	0.104	179.042
Measured device	907.998	11.531	-95.123	0.021	0.099	179.084
Deviation	0.013	0.048	-0.290	0.003	0.005	-0.042

measured values of the precision measurement device and measured values from the developed measurement device. As presented in Table 2, the measurement results reveal that the standard deviation is within 0.294 mm, which satisfies the measurement error criterion.

## 6. Conclusions

This study proposed a spatial location measurement device and method for the synchronization of a virtual environment and a stable multi-screen frame structure to implement the multi-screen-based visualization environment, and the following conclusions were made.

1. An efficient and safe multi-screen frame structure could be designed that could be installed portably.
2. The basis of the technology for a VR display environment using a multi-screen structure could be obtained through the reliability verification of the real screen measurement method and an algorithm for synchronization between real and virtual spaces.
3. Compared to expensive precision measurement devices, an efficient measurement device was developed that can obtain comparable measurement results, and the reliability was verified.
4. This study proposed an efficient method for synchronization between virtual and real spaces, through which an alternative to the existing HMD-based VR visualization environment and system was presented. These results will be utilized to propose new directions in VR application fields in the future.

## Acknowledgments

This study was supported by the “Technical Development Project of 2017 Digital Contents (VR/AR/MR) Flagship (Project Number: 20170017830 022002)” of the Ministry of Science and ICT and the Institute for Information and Communications Technology Promotion.

## REFERENCES

1. Carolina, C. N., Daniel, J. S. and Thomas, A. D., “Surround-screen projection-based virtual reality: the design and implementation of the CAVE,” Proc. of the 20th annual conference on Computer graphics and interactive techniques, pp. 135-142, 1993.
2. Fung, J., Richards, C. L., Malouin, F., McFadyen, B. J. and Lamontagne, A., “A treadmill and motion coupled virtual reality system for gait training post-stroke,” *Cyberpsychology & behavior*, Vol. 9, No. 2, pp. 157-219, 2006.
3. Moon, D. J., Cho, J. H., Choi, Y. S., Hwang, I. H. and Lee, J. C., “High-Stiffness Structure Design of 8-Axis Multi-tasking Machine for Automotive Powertrain Shafts,” *Journal of the Korean Society of Manufacturing Process Engineers*, Vol. 15, No. 2, pp. 78-83, 2016.
4. Chun, C. U., Park, S. B. and Song, J. I., “Study on the Load Analysis in Accordance with the Contact Position between a High-Load Long-Pitch Roller Chain and Sprocket,” *Journal of the Korean Society of Manufacturing Process Engineers*, Vol. 16, No. 1, pp. 51-57, 2017.
5. Kim, H. M., Kim, L. S., Cho, S. H. and Lyu, S. K., “A study on the design and performance test of side thruster,” *Journal of the Korean Society of Manufacturing Process Engineers*, Vol. 16, No. 2, pp. 1-6, 2017.
6. Kwon, Y. J. and Shreepud, R., “E-Quality for Manufacturing(EQM) within the Framework of Internet-based Systems,” *IEEE Transactions on System*, Vol. 37, No. 6, pp. 1365-1372, 2007.

7. Chai, X. and Yang, Q., "Reducing the calibration effort for probabilistic indoor location estimation," IEEE Transactions on Mobile Computing, Vol. 6, No. 6, pp. 649-662, 2007.
8. Kenneth, L. C., Elad, H. and David, P. W., "Sublinear optimization for machine learning," Journal of the ACM, Vol. 59, No. 5, pp. 1-49, 2012.